

Influence of the pK_a value of the buried, active-site cysteine on the redox properties of thioredoxin-like oxidoreductases

Ekkehard Mössner¹, Hideo Iwai¹, Rudi Glockshuber*

Institut für Molekularbiologie und Biophysik, Eidgenössische Technische Hochschule Hönggerberg, CH-8093 Zürich, Switzerland

Received 8 May 2000

Edited by Giorgio Semenza

Abstract Thioredoxin constitutes the prototype of the thiol-disulfide oxidoreductase family. These enzymes contain an active-site disulfide bridge with the consensus sequence Cys-Xaa-Xaa-Cys. The more N-terminal active-site cysteine is generally a strong nucleophile with an abnormal low pK_a value. In contrast, the more C-terminal cysteine is buried and only little is known about its effective pK_a during catalysis of disulfide exchange reactions. Here we have analyzed the pK_a values of the active-site thiols in wild type thioredoxin and a 400-fold more oxidizing thioredoxin variant by NMR spectroscopy, using selectively $^{13}C^\beta$ -Cys-labeled proteins. We find that the effective pK_a of the buried cysteine (pK_N) of the variant is increased, while the pK_a of the more N-terminal cysteine (pK_C) is decreased relative to the corresponding pK_a values in the wild type. We propose two empirical models which exclusively require the knowledge of pK_N to predict the redox properties of thiol-disulfide oxidoreductases with reasonable accuracy. © 2000 Federation of European Biochemical Societies. Published by Elsevier Science B.V. All rights reserved.

Key words: Thiol-disulfide oxidoreductase; Thioredoxin; Redox potential; pK_a value; Disulfide exchange reaction

1. Introduction

Thiol-disulfide oxidoreductases of the thioredoxin (Trx) family are structurally related proteins which share the so-called Trx fold. These enzymes contain a catalytic disulfide bond in their active site which is located at the N-terminus of the first α -helix in the Trx motif and has the consensus sequence Cys-Xaa-Xaa-Cys (for reviews, see [1,2]). Despite many similarities in primary and tertiary structure, large differences in redox potentials are observed between individual members of the thiol-disulfide oxidoreductase family. It has become clear that the Xaa-Xaa dipeptide between the active-site cysteines is an important determinant of the redox potential, and that there is a correlation between the redox potential and the abnormal low pK_a value of the N-terminal active-site thiol group that acts as nucleophile during catalysis of disul-

fide exchange reactions [3–5]. In the most oxidizing member of the Trx family, DsbA from *Escherichia coli* ($E_o' = -122$ mV), the pK_a of the nucleophilic cysteine is approximately 3.5, i.e. 6 pK_a units below the pK_a of a normal cysteine thiol (~ 9.5). In the most reducing member of the family, *E. coli* Trx ($E_o' = -270$ mV), the pK_a of the nucleophilic thiol is much higher (7.0–7.5), but still below the normal pK_a value of a cysteine thiol. Several explanations for the lowered pK_a of the nucleophilic thiol group have been proposed such as an electrostatic interaction between the thiolate anion and the dipole of the active-site helix, hydrogen bonding between the thiolate and main chain amide groups of the active-site helix, a shared proton between both active-site cysteines and, in the case of DsbA and eukaryotic protein disulfide isomerase (PDI), an electrostatic interaction with a histidine side chain preceding the second cysteine residue [6–9].

The pK_a values of the nucleophilic thiols in thiol-disulfide oxidoreductases have been correlated quantitatively with their redox potentials by applying the Brønsted theory that allows prediction of pH-dependent rate constants of intermolecular disulfide exchange reactions [3–5,10]. Such a prediction requires the knowledge of the pK_a values of all three thiol groups involved in a disulfide exchange reaction, i.e. the nucleophilic, the central and the leaving group thiol [11]. The redox potentials of thiol-disulfide oxidoreductases are generally deduced from their equilibrium constants with reduced (GSH) and oxidized glutathione (GSSG). As the more C-terminal active-site cysteine of these enzymes is buried and does not form mixed disulfides with substrates, the overall equilibrium between the enzyme, e.g. Trx, and glutathione is determined by four microscopic rate constants (k_1 – k_4) according to the following scheme [10]:



Consequently, the prediction of the overall equilibrium constant depends on the accurate prediction of the four individual rate constants k_1 – k_4 which, as mentioned above, depend on the pK_a values of both active-site cysteines.

Many experimental techniques such as chemical modifications and nuclear magnetic resonance (NMR), Raman and UV-absorbance spectroscopy [12–16] have been applied to determine the pK_a values of the active-site cysteines in *E. coli* Trx. It was found that the pK_a of the nucleophilic cysteine (Cys-32) is approximately 7.0–7.5, while there is still uncertainty about the pK_a of the buried active-site cysteine (Cys-35) [12,14–17]. Specifically, it is not known whether the pK_a of Cys-35 is shifted in active-site variants of Trx that show an increased redox potential and a decreased pK_a of Cys-32.

*Corresponding author. Fax: (41)-1-633 1036.
E-mail: rudi@mol.biol.ethz.ch

¹ Present address: Biochemisches Institut der Universität Zürich, Winterthurerstrasse 190, CH-8057 Zürich, Switzerland.

Here, we have employed selective $^{13}\text{C}^\beta$ -Cys labeling of Trx to determine the pK_a of the buried active-site cysteine (Cys-35) by ^{13}C -NMR spectroscopy. In addition, we have investigated the pK_a of Cys-35 in the most oxidizing Trx variant known so far ($E_o' = -195$ mV). This variant bears the Xaa-Xaa dipeptide sequence of glutaredoxin (Pro-Tyr), and the pK_a of the nucleophilic Cys-32 is lowered to 5.9 [5]. We provide experimental evidence for inversely shifted pK_a values of the two active-site cysteines in this variant relative to the cysteine pK_a values in the wild type. Based on this observation, we propose an empirical model for predicting the redox potentials of thiol-disulfide oxidoreductases which exclusively requires the knowledge of the pK_a of the more N-terminal, active-site cysteine. We also present a second model in which the pK_a of the buried, active-site cysteine is assumed to be invariant in all Trx-like oxidoreductases. Both models are in good agreement with the known redox properties of Trx-like thiol-disulfide oxidoreductases.

2. Materials and methods

2.1. Materials

$^{13}\text{C}^\beta$ -labeled cystine was purchased from Cambridge Isotope Laboratories. Amino acids, salts for growth media and iodoacetamide were from Sigma and Merck (Darmstadt, Germany). Isopropyl- β -D-thiogalactoside (IPTG) was from AxonLab (Buchs, Switzerland). All other chemicals were of analysis grade.

2.2. Purification of selectively $^{13}\text{C}^\beta$ -labeled Trxs

The T7 expression plasmids for Trx wild type (pTrx) and the glutaredoxin-like variant (pTrx(PY)) [5] were used to transform BL21(DE3)cysE51 cells [18] for selective isotopic labeling. Overnight cultures were grown in rich medium (LB) supplemented with 100 mg/l ampicillin and used to inoculate the final growth medium by a 1/100 dilution. Specific $^{13}\text{C}^\beta$ labeling of the cysteines was performed according to the following procedures.

Method 1: a synthetic rich medium was prepared essentially as described [19,20], containing the following compounds (per liter of medium): KH_2PO_4 , 7.8 g; K_2HPO_4 , 4.0 g; citric acid monohydrate, 1.0 g; NH_4Cl , 1.0 g. The pH was adjusted to 7.2 with NaOH and the medium was autoclaved. Afterwards, amino acids, nucleosides, vitamins and glucose were added (amino acids: Ser, 1.6 g; Ala, Gln, Glu, Arg and Gly, 400 mg each; Asn and Met, 250 mg each; His, Ile, Leu, Lys, Asn, Pro, Thr, Val and Tyr, 100 mg each; Trp, 50 mg; nucleosides: cytosine, guanosine and uracil, 125 mg each; thymine 50 mg; nicotinic acid, 50 mg; thiamine, 50 μg ; biotin, 100 μg ; glucose, 10 g). Unlabeled cysteine and cystine were omitted and $^{13}\text{C}^\beta$ -labeled cystine (50 mg/l) was added instead. After inoculation, cells were grown at 37°C to an optical density at 660 nm (OD_{660}) of ~ 1.0 and induced with IPTG (final concentration: 1 mM). A second portion of $^{13}\text{C}^\beta$ -labeled cystine (50 mg/l) was added simultaneously. Cells were grown further for 3–4 h and harvested by centrifugation.

Method 2: the labeling medium and growth conditions were the same as in method 1, except that 20 mg/l unlabeled cysteine was used for growth until an OD_{660} of 0.5 was reached. Then a single portion of $^{13}\text{C}^\beta$ -labeled cystine (50 mg/l) was added. Protein expression was induced with IPTG 30 min later. Further growth was performed as in method 1.

$^{13}\text{C}^\beta$ -Cys-labeled Trx wild type and the labeled [PY]-variant were purified exactly as described previously [5], with final yields of 80 mg purified protein per liter of bacterial culture using method 1 and 40 mg/l using method 2. Protein concentrations were determined by the specific absorbance at 280 nm ($A_{280\text{ nm}, 0.1\%, 1\text{ cm}}$) with values of 1.24 for Trx wild type and 1.37 for [PY]-Trx [5].

2.3. Preparation of the mono-alkylated forms of unlabeled and $^{13}\text{C}^\beta$ -Cys-labeled Trxs

Trx (100 μM) was incubated with 50 mM dithiothreitol (DTT) at pH 7.0 and 25°C for 2 h and separated from excess DTT by gel filtration (PD10, Pharmacia). The reduced proteins (80 μM) were incubated with 5 mM iodoacetamide at pH 7.0 and 25°C for 30 min and

then extensively dialyzed against distilled water. Mass spectra of the reaction products showed that the mono-alkylated proteins were obtained with a yield of >95%.

2.4. Circular dichroism (CD) spectra

CD spectra were recorded at 25°C on a JASCO-710 spectrometer using quartz cuvettes of 0.1 cm pathlength. Protein concentrations were 30 μM . The pH-dependent stability of the proteins was determined between pH 4 and pH 12 using a buffer system containing 20 mM boric acid and 20 mM sodium phosphate adjusted to the desired pH by addition of NaOH or HCl. Proteins were incubated at the corresponding pH for 3 h before the measurements. Far-UV CD spectra were measured between 250 and 190 nm. Alternatively, the molar mean residue ellipticity was recorded at a constant wavelength of 218 nm for 3 min.

2.5. NMR measurements

Protein concentrations were 0.2–0.5 mM in 25 mM sodium phosphate pH 7.0, dissolved in 90% $\text{H}_2\text{O}/10\%$ D_2O . All measurements were performed on a Varian INOVA 400 spectrometer operating at a ^1H frequency of 400 MHz with a triple resonance probe head equipped with Z gradient coil. The ^{13}C chemical shifts were calibrated to the reference (DSS) indirectly [21]. A series of ^{13}C -HSQC spectra was recorded at 298 K after adjusting the respective pH by addition of minute amounts of HCl or NaOH. In the experiments with reduced Trxs, DTT was added to a final concentration of 5 mM. The pH of the sample was verified before and after each measurement. All spectra were processed with the program PROSA [22] and analyzed using the program XEASY [23].

2.6. Resonance assignments

The assignments of the $^{13}\text{C}^\beta$ resonances of the cysteines in Trx wild type were straightforward because Trx only contains two cysteines so that only two strong resonances were observed for the $^{13}\text{C}^\beta$ -Cys-labeled proteins. We assigned each $^{13}\text{C}^\beta$ resonance from the two cysteines based on the previously reported assignments [24,25]. Upon alkylation of Trx wild type and [PY]-Trx at Cys-32 with iodoacetamide, only one of the two $^{13}\text{C}^\beta$ -Cys resonances in each protein showed a large chemical shift (from 27.2 to 35.5 ppm in the wild type and from 31.2 to 37.2 ppm in [PY]-Trx at pH 7.0). The shifted resonances were therefore assigned to $^{13}\text{C}^\beta$ of Cys-32.

2.7. Evaluation of pH titration profiles

Plots of chemical shifts (δ) as a function of pH were fitted using the program KaleidaGraph (Abelbeck Software) using the following equations [7,17]. For simple titrations involving only one pK_a value, Eq. 2 was used where δ_{HA} and δ_{A} are the chemical shifts of the fully protonated and unprotonated forms, respectively.

$$\delta(\text{pH}) = \delta_{\text{HA}} \frac{(\delta_{\text{HA}} - \delta_{\text{A}})}{1 + 10^{(\text{pK}_a - \text{pH})}} \quad (2)$$

In those cases where the baselines of the chemical shifts before and after the titration were pH-dependent, Eq. 3 was used to fit the data.

$$\delta(\text{pH}) = (m_{\text{HA},o} \cdot \text{pH} + \delta_{\text{HA},o}) - \frac{(m_{\text{HA},o} \cdot \text{pH} + \delta_{\text{HA},o}) - (m_{\text{A},o} \cdot \text{pH} + \delta_{\text{A},o})}{1 + 10^{(\text{pK}_a - \text{pH})}} \quad (3)$$

Here, $\delta_{\text{HA},o}$ and $\delta_{\text{A},o}$ are the chemical shift values of the fully protonated and unprotonated form, respectively, at pH 0. $m_{\text{HA},o}$ and $m_{\text{A},o}$ are the slopes describing the linear dependency of the chemical shifts on pH.

Eq. 4 describes a titration with two pK_a values where δ_{HAH} denotes the chemical shift of the doubly protonated form.

$$\delta(\text{pH}) = \frac{\delta_{\text{HAH}} + \delta_{\text{HA}} \cdot 10^{\text{pH} - \text{pK}_1} + \delta_{\text{A}} \cdot 10^{(2\text{pH} - \text{pK}_1 - \text{pK}_2)}}{10^{2\text{pH} - \text{pK}_1 - \text{pK}_2} + 1 + 10^{(\text{pH} - \text{pK}_1)}} \quad (4)$$

2.8. Correlation between the equilibrium constant with glutathione and the pK_a values of active-site cysteines

The equilibrium between Trx and glutathione can be described by Eq. 1 with four different rate constants (k_1 – k_4) for the individual microscopic disulfide exchange reactions [10]. The equilibrium constant ($K_{\text{GSH/GSSG}}$) can be expressed by Eq. 5 on the basis of the concentrations of the individual compounds at equilibrium, or by

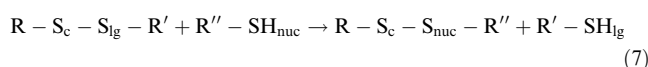
Eq. 6 on the basis of all individual rate constants contributing to this equilibrium.

$$K_{\text{GSH/GSSG}} = \frac{[\text{Trx}_S^{\text{SH}}] \cdot [\text{GSH}]^2}{[\text{Trx}_{\text{SH}}^{\text{SH}}] \cdot [\text{GSSG}]} \quad (5)$$

$$K_{\text{GSH/GSSG}} = \frac{k_1 \cdot k_3}{k_2 \cdot k_4} \quad (6)$$

The individual rate constants k_1 – k_4 at a given pH can be predicted according to [11] by applying the Brønsted theory on general acid/base catalysis to disulfide exchange reactions. As a prerequisite, the $\text{p}K_a$ values of all thiol compounds involved have to be known. In addition, prediction of the first-order rate constant k_3 requires the knowledge of the effective concentration of the Cys-35 thiol, which is however unknown. A value of 1 M was used in all calculations, which yielded reasonable values for the predicted overall equilibrium constants [3–5,10]. A value of 8.7 was used for the $\text{p}K_a$ of the thiol in glutathione in all calculations.

A general reaction scheme for disulfide exchange reactions is depicted in Eq. 7, where the terms ‘nuc’, ‘c’ and ‘lg’ refer to nucleophilic, central and leaving group sulfur, respectively.



The apparent rate constant (k) for each individual disulfide exchange reaction at a given pH is described by Eq. 8 [11].

$\log k =$

$$(6.3 + 0.59 \cdot \text{p}K_{a,\text{nuc}} - 0.40 \cdot \text{p}K_{a,\text{c}} - 0.59 \cdot \text{p}K_{a,\text{lg}}) - \log(1 + 10^{\text{p}K_{a,\text{nuc}} - \text{pH}}) \quad (8)$$

Combination of all calculated values of k_1 – k_4 using Eq. 6, and assuming an effective concentration of 1 M for Cys-35 for calculating k_3 yields $K_{\text{GSH/GSSG}}$ at each pH value (see Section 3). It is important to note that the relevant $\text{p}K_a$ of Cys-35 for predicting k_3 is the $\text{p}K_a$ of Cys-35 that is observed when Cys-32 has formed a mixed disulfide, and not the $\text{p}K_a$ of Cys-35 in reduced Trx.

3. Results and discussion

3.1. Production of $^{13}\text{C}^\beta$ -Cys-labeled Trxs

Trx wild type and its glutaredoxin-like variant with the Xaa-Xaa sequence Pro-Tyr ([PY]-Trx), specifically labeled at the $^{13}\text{C}^\beta$ positions of both active-site cysteines, were cytoplasmically expressed and purified with high yields (40–80 mg homogeneous protein per liter of bacterial culture) using the T7 expression system in the cysteine auxotroph *E. coli* strain BL21(DE3)cysE51 [18] (see Section 2).

3.2. pH titration of reduced wild type and [PY]-Trx by ^{13}C -NMR

The $^{13}\text{C}^\beta$ -labeled cysteines allowed the pH titration of the thiols of Cys-32 and Cys-35 of Trx wild type and the PY-variant by following the corresponding $^{13}\text{C}^\beta$ resonances. Titrations of wild type Trx and [PY]-Trx were carried out in the reduced and oxidized state (Table 1). The pH dependence of the ^{13}C chemical shifts of the C^β atoms of Cys-32 and Cys-35 of reduced wild type Trx and [PY]-Trx is shown in Fig. 1. The reduced wild type showed the same transition pattern for the $^{13}\text{C}^\beta$ resonance of Cys-32 as reported before [12], and it is widely accepted that the first transition in the curve for $^{13}\text{C}^\beta$ of Cys-32 in reduced wild type Trx, having a $\text{p}K_a$ of 7.2, corresponds to the $\text{p}K_a$ of Cys-32 [12,13,17]. In contrast, the $\text{p}K_a$ of Cys-35 in reduced wild type Trx is not evident from the titration data. The titration profile of Cys-35 shows a smaller amplitude and is similar to that of Cys-32. This has been interpreted such that the pH dependence of the $^{13}\text{C}^\beta$ chemical shift of Cys-35 between pH 3 and 10 reflects the ionization of the neighboring Cys-32 thiol and not the ionization of the Cys-35 thiol itself [24].

Reduced Trx wild type shows two down-field transitions for both cysteine $^{13}\text{C}^\beta$ resonances with increasing pH (Fig. 1A). Reduced [PY]-Trx, in contrast, shows just one down-field transition for Cys-32 and Cys-35 with a $\text{p}K_a$ of 6.0 and no second transition (Fig. 1B). In addition, the pre- and post-translational baselines of the $^{13}\text{C}^\beta$ chemical shifts in [PY]-Trx were pH-dependent. Therefore, baseline slopes were included as additional variables for the evaluation of the chemical shift data. As in wild type Trx, the $^{13}\text{C}^\beta$ signal of Cys-35 in [PY]-Trx yielded a similar $\text{p}K_a$ as the Cys-32 titration, but a smaller amplitude. Thus, the chemical shift change of $^{13}\text{C}^\beta$ of Cys-35 in the variant was also attributed to the ionization of Cys-32.

3.3. ^{13}C -NMR pH titration of alkylated wild type and [PY]-Trx

The overall disulfide exchange mechanism between Trx and glutathione (Eq. 1) shows that it is not the $\text{p}K_a$ value of Cys-35 in reduced Trx that is relevant for the equilibrium, but the $\text{p}K_a$ value of Cys-35 when Cys-32 has formed a mixed disulfide with glutathione. However, the mixed disulfide between Trx and glutathione is kinetically unstable and not directly accessible for titration experiments. In order to mimic the Trx/glutathione mixed disulfide, we used chemically modified forms of wild type and [PY]-Trx in which Cys-32 was selectively alkylated with iodoacetamide [5,24]. Alkylation of Cys-

Table 1
pH dependence of the $^{13}\text{C}^\beta$ chemical shifts of Cys-32 and Cys-35 in Trx wild type and [PY]-Trx

Covalent structure		Oxidized		Reduced		Alkylated	
protein	atom	$\text{p}K_a$	$\Delta\delta$ (ppm) ^a	$\text{p}K_a$	$\Delta\delta$ (ppm) ^a	$\text{p}K_a$	$\Delta\delta$ (ppm) ^a
wild type Trx	$^{13}\text{C}^\beta$ -Cys-32	$7.32 \pm 0.05^{\text{d}}$	−0.2	7.23 ± 0.04	+1.2	$7.59 \pm 0.09^{\text{b,d}}$	
	$^{13}\text{C}^\beta$ -Cys-35	$7.45 \pm 0.16^{\text{b,d}}$		$9.53 \pm 0.04^{\text{d}}$	+2.0		
[PY]-Trx	$^{13}\text{C}^\beta$ -Cys-32	$7.32 \pm 0.10^{\text{d}}$	−0.2	$7.62 \pm 0.14^{\text{d}}$	+0.4	$7.00 \pm 0.12^{\text{d}}$	−0.2
				$9.77 \pm 0.15^{\text{d}}$	+0.7	$11.1 \pm 0.02^{\text{c}}$	+2.0 ^c
	$^{13}\text{C}^\beta$ -Cys-35	$7.68 \pm 0.09^{\text{d}}$	+0.2	$5.97 \pm 0.12^{\text{b}}$		$7.13 \pm 0.03^{\text{d}}$	−0.8
				$6.02 \pm 0.16^{\text{b,d}}$		$11.8 \pm 0.04^{\text{c}}$	+2.0 ^c

^aOverall amplitude of the pH-dependent ^{13}C chemical shift change.

^bA linear dependence of the pre- and post-translational baselines on pH was assumed for fitting the data according to an acid/base equilibrium (Eq. 3). $\Delta\delta$ is not indicated in the case of pH-dependent baselines.

^c $\Delta\delta$ was assumed to be 2.0 ppm for the calculation of the $\text{p}K_a$ values of Cys-32 in the alkylated proteins [24,26].

^dApparent $\text{p}K_a$, reflecting the titration of side chains in the vicinity of Cys-32 and Cys-35.

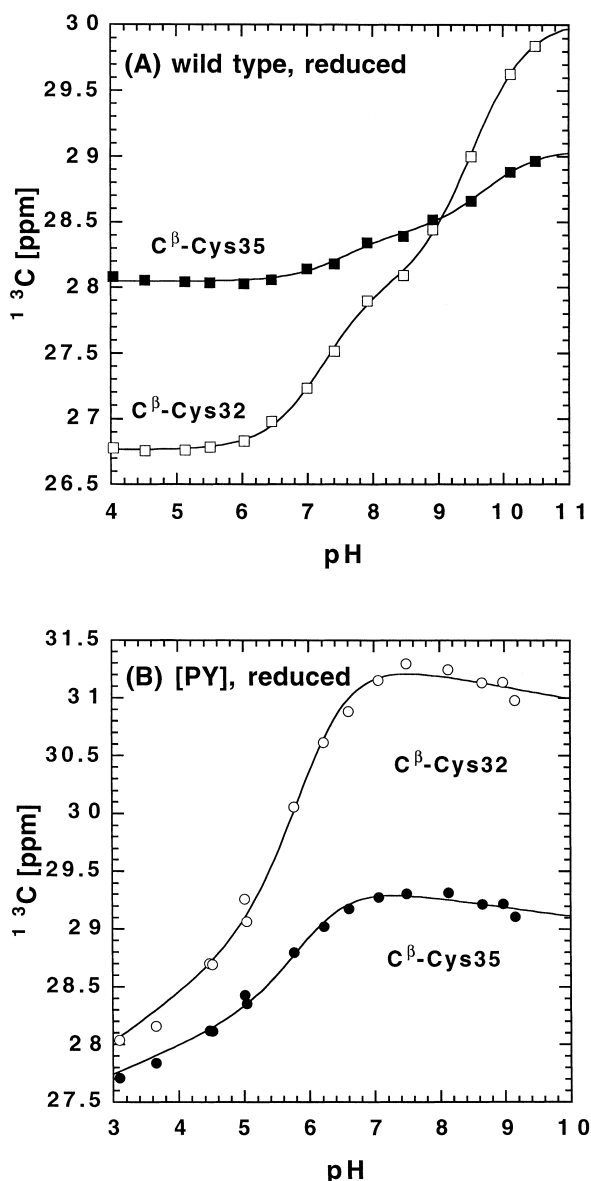


Fig. 1. Dependence on pH of the ^{13}C chemical shifts of the C^{β} atoms of Cys-32 and Cys-35 in reduced *E. coli* Trx, measured at 298 K. (A) wild type Trx. (B) [PY]-Trx. Filled and open symbols indicate the $^{13}\text{C}^{\beta}$ resonances of Cys-35 and Cys-32, respectively. The solid lines in A are obtained by fitting the data to Eq. 3 and the curves in B were obtained by fitting the data to Eq. 2 (see Section 2).

32, like formation of the mixed disulfide, removes the pH-dependent negative charge at Cys-32 and should thus provide a reasonable model for determination of the microscopic pK_a value of Cys-35 in the Trx/glutathione mixed disulfide.

An up-field titration of $^{13}\text{C}^{\beta}$ for Cys-32 with a pK_a of 7.6 in alkylated wild type Trx has been reported previously [24]. We observed similar up-field shifts for the $^{13}\text{C}^{\beta}$ resonances of the alkylated Cys-32 in [PY]-Trx and wild type Trx (Fig. 2B). This titration has previously been assigned to the ionization of the neighboring Asp-26 side chain [24]. Importantly, clear differences between alkylated [PY]- and alkylated wild type Trx are observed at higher pH values for the $^{13}\text{C}^{\beta}$ resonances of Cys-35 (Fig. 2A). A large down-field shift starting around pH 10 is observed for Cys-35 in alkylated wild type Trx. The transition

yielded a pK_a of 11.1 when a titration amplitude of 2.0 ppm for the cysteine $^{13}\text{C}^{\beta}$ resonance was assumed [24,26]. Alkylated [PY]-Trx also showed a slight down-field shift of Cys-35, but at significantly higher pH (Fig. 2A). Assuming the same amplitude of 2.0 ppm for the titration, a pK_a of Cys-35 of about 11.8 is obtained. Although both transitions could not be measured completely due to denaturation problems, the NMR titration data demonstrate that the pK_a of Cys-35 in alkylated [PY]-Trx is increased compared to that in the alkylated wild type, while the pK_a of Cys-32 is lowered in the variant compared to the wild type ([5], Table 1).

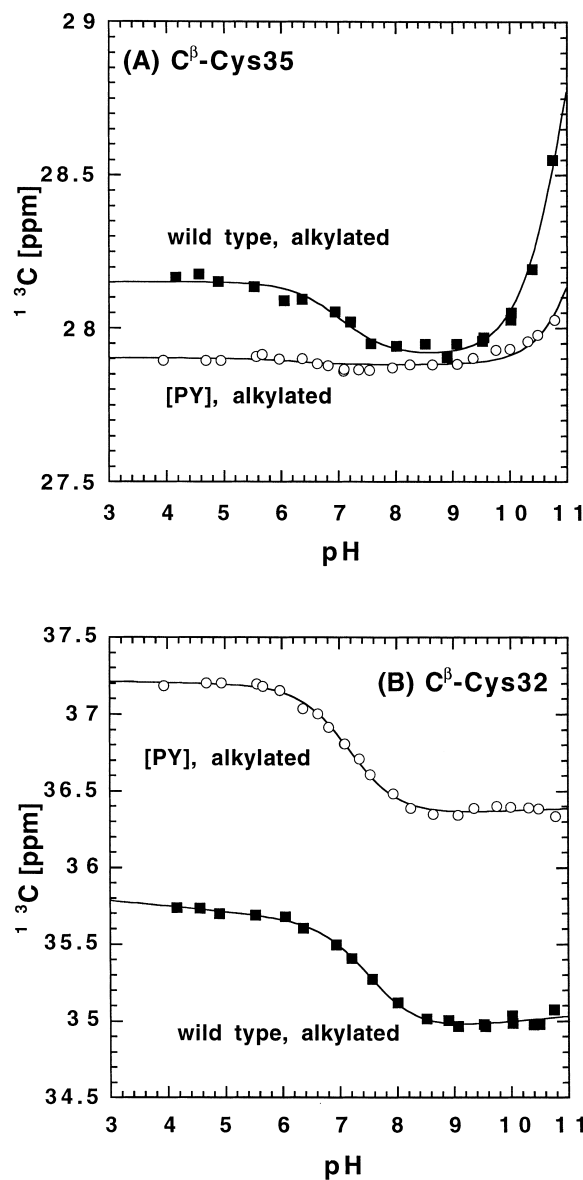


Fig. 2. Dependence on pH of the ^{13}C chemical shifts of the C^{β} atoms of Cys-32 and Cys-35 in *E. coli* Trx after alkylation of the solvent-accessible cysteine thiol (Cys-32) with iodoacetamide in order to mimic a mixed disulfide intermediate that occurs in the equilibrium with glutathione. (A) $^{13}\text{C}^{\beta}$ resonances of Cys-35, (B) $^{13}\text{C}^{\beta}$ resonances of Cys-32. Open circles and filled rectangles indicate [PY]- and wild type Trx, respectively.

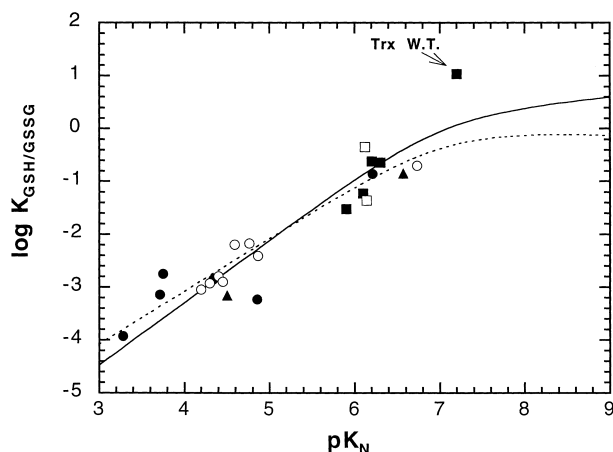


Fig. 3. Plots of the equilibrium constants with glutathione ($K_{\text{GSH/GSSG}}$) versus the $\text{p}K_{\text{a}}$ values of the nucleophilic, active-site cysteines ($\text{p}K_{\text{N}}$) of different thiol-disulfide oxidoreductases and variants thereof. (■) Trx variants from [5]; (□) Trx variants from [17]; (●) and (○) DsbA variants described in [4] and [3], respectively. Two variants of the isolated human PDI *a*-domain [9] are also included (▲). Two different theoretical models were applied to fit the experimental data on the basis of the Brønsted theory for prediction of rate constants of disulfide exchange reactions [11] (cf. Eqs. 1 and 5–8), and assuming an effective concentration of 1 M of the buried, active-site cysteine. The solid line corresponds to a fit according to Eq. 10 where it is assumed that the $\text{p}K_{\text{a}}$ value of the buried, active-site cysteine ($\text{p}K_{\text{b}}$) is invariant in all Trx-like oxidoreductases. The fit yields a value of 11.7 ± 0.5 for $\text{p}K_{\text{b}}$ (correlation coefficient: 0.930). The second model (dashed line) assumes that the sum of the $\text{p}K_{\text{a}}$ values of the active-site cysteines of thiol-disulfide oxidoreductases is constant (i.e. inversely shifted values of $\text{p}K_{\text{N}}$ and $\text{p}K_{\text{b}}$). The fit yields $\text{p}K_{\text{N}} + \text{p}K_{\text{b}} = 16.9 \pm 0.5$ (correlation coefficient: 0.928). Wild type Trx (arrow) exhibits the strongest deviation from both models.

3.4. Models for predicting the redox potential of thiol-disulfide oxidoreductases from the $\text{p}K_{\text{a}}$ value of their nucleophilic, active-site cysteine

Fig. 3 shows the reported equilibrium constants with glutathione (K_{eq}) of active-site variants of DsbA, the PDI *a*-domain, and Trx as a function of the $\text{p}K_{\text{a}}$ of the more N-terminal, nucleophilic active-site cysteine. Using these data and assuming an effective concentration of 1 M for the buried, active-site cysteine to calculate the first-order rate constant k_3 (cf. Eqs. 1, 6 and 8), two empirical models for predicting the redox properties of thiol-disulfide oxidoreductases were tested that exclusively require the knowledge of the $\text{p}K_{\text{a}}$ of the nucleophilic, active-site cysteine thiol.

Combination of Eqs. 1 and 5–8 yields the general Eq. 9 for calculating the overall equilibrium constant K_{eq} of the redox equilibrium between a thiol-disulfide oxidoreductase and an organic monothiol compound, where $\text{p}K_{\text{N}}$ is the $\text{p}K_{\text{a}}$ of the more N-terminal, exposed active-site cysteine, $\text{p}K_{\text{b}}$ is the $\text{p}K_{\text{a}}$ of the buried active-site cysteine when the exposed cysteine has formed a mixed disulfide, and $\text{p}K_{\text{T}}$ is the $\text{p}K_{\text{a}}$ of the organic monothiol:

$$\log K_{\text{eq}} = 1.18 \cdot (\text{p}K_{\text{N}} + \text{p}K_{\text{b}} - 2\text{p}K_{\text{T}}) + 2 \cdot \log (1 + 10^{\text{p}K_{\text{T}} - \text{pH}}) - \log (1 + 10^{\text{p}K_{\text{N}} - \text{pH}}) - \log (1 + 10^{\text{p}K_{\text{b}} - \text{pH}}) \quad (9)$$

Using standard conditions ($\text{pH} = 7.0$) and glutathione as the reference thiol compound ($\text{p}K_{\text{T}} = 8.7$) [11], the predicted equi-

librium between a thiol-disulfide oxidoreductase and glutathione ($K_{\text{GSH/GSSG}}$) at $\text{pH} 7.0$ is given by Eq. 10.

$$\log K_{\text{GSH/GSSG}} = 1.18 \cdot (\text{p}K_{\text{N}} + \text{p}K_{\text{b}} - 17.4) + 3.417 - \log (1 + 10^{\text{p}K_{\text{N}} - 7}) - \log (1 + 10^{\text{p}K_{\text{b}} - 7}) \quad (10)$$

Using Eq. 10, we then compared two different theoretical models for their agreement with the experimentally determined pairs of K_{eq} and $\text{p}K_{\text{N}}$ of different thiol-disulfide oxidoreductases (see Fig. 3). In model 1, it was assumed that $\text{p}K_{\text{b}}$ is invariant in all thiol-disulfide oxidoreductases. The fit yielded a value of 11.7 ± 0.5 for $\text{p}K_{\text{b}}$ (correlation coefficient 0.930) (Fig. 3, solid line). Eq. 11 uses $\text{p}K_{\text{b}} = 11.7$ and predicts $K_{\text{GSH/GSSG}}$ at $\text{pH} 7.0$ for any thiol-disulfide oxidoreductase, exclusively on the basis of its $\text{p}K_{\text{N}}$.

$$\log K_{\text{GSH/GSSG}} = 1.18 \cdot (\text{p}K_{\text{N}} - 5.73) - \log (1 + 10^{\text{p}K_{\text{N}} - 7}) - 1.253 \quad (11)$$

Eq. 11 proved to predict the known values of $K_{\text{GSH/GSSG}}$ (cf. Fig. 3) reasonably well. All measured values of $K_{\text{GSH/GSSG}}$ deviated by less than a factor of 10 from the theoretical values. Combination of Eq. 11 with the Nernst equation and the standard redox potential of glutathione ($E_{\text{o}}'_{\text{GSH/GSSH}} = -240$ mV; [27]) yields the general Eq. 12 for predicting the intrinsic redox potential of a thiol-disulfide oxidoreductase (E_{o}') at 25°C and $\text{pH} 7.0$ with an accuracy of ± 30 mV:

$$E_{\text{o}}' = -0.240 \text{ V} - 0.0296 \text{ V} \cdot (1.18 \cdot (\text{p}K_{\text{N}} - 5.73) - \log (1 + 10^{\text{p}K_{\text{N}} - 7}) - 1.253) \quad (12)$$

As we had observed an inverse shift of the $\text{p}K_{\text{a}}$ values of the active-site cysteines in [PY]-Trx compared to Trx wild type, we also tested another theoretical model in which it was assumed that the sum of $\text{p}K_{\text{N}}$ and $\text{p}K_{\text{b}}$ is the same in all thiol-disulfide oxidoreductases, corresponding to the possibility of inversely shifted $\text{p}K_{\text{a}}$ values instead of a constant value of $\text{p}K_{\text{b}}$ (cf. [3,9,28]). Fitting the data in Fig. 3 with Eq. 10 yielded $\text{p}K_{\text{N}} + \text{p}K_{\text{b}} = 16.9 \pm 0.5$ (correlation coefficient: 0.928) (Fig. 3, dashed line). Again, none of the calculated values of $K_{\text{GSH/GSSG}}$ differed by more than 10-fold from the measured values, except for that of Trx wild type, where the experimental value is 22-fold higher than the calculated one. It is at present not clear whether this is just an outlier or whether the whole concept of a linkage between thiol $\text{p}K_{\text{a}}$ value and redox potential breaks down in wild type Trx [28].

Eqs. 13 and 14 allow the prediction of $K_{\text{GSH/GSSG}}$ and E_{o}' of a thiol-disulfide oxidoreductase according to model 2:

$$\log K_{\text{GSH/GSSG}} = 2.79 - \log (1 + 10^{\text{p}K_{\text{N}} - 7}) - \log (1 + 10^{9.9 - \text{p}K_{\text{N}}}) \quad (13)$$

$$E_{\text{o}}' = -0.240 \text{ V} - 0.0296 \text{ V} \cdot (2.79 - \log (1 + 10^{\text{p}K_{\text{N}} - 7}) - \log (1 + 10^{9.9 - \text{p}K_{\text{N}}})) \quad (14)$$

The Eqs. 12 and 14 predict the redox potentials of thiol-disulfide oxidoreductases with remarkable accuracy (± 30 mV). In both models, a very low effective concentration (1 M) of the buried active-site cysteine during the intramolecular

reaction (k_3) is assumed, and both models, in accordance with the experimental data, yield abnormal, high values for pK_b . The reactivity of the buried cysteine thus indeed appears to be very low at physiological pH. This was indeed observed for glutaredoxin and DsbA, where the activities of the wild type enzymes were only slightly reduced during catalysis of disulfide exchange reactions when their buried active-site cysteines were replaced [29,30]. Nevertheless, low effective concentrations of the buried thiols in Trx-like enzymes are quite unexpected, because rate enhancements for intramolecular reactions are very substantial, and effective concentrations are reported to be as high as 10^2 M for disulfide interchange reactions between organic compounds, 10^5 M for disulfide bonds in proteins [31] and up to 10^9 M for the intramolecular formation of organic anhydrides [32].

The described empirical models for the interrelation between the redox potentials and the values of pK_N of Trx-type oxidoreductases may be used in the future for predicting the function of newly discovered members of this enzyme family, and for selecting an appropriate catalyst for disulfide exchange reactions and oxidative protein folding under given conditions in vitro.

Acknowledgements: We thank Prof. K. Wüthrich for continuous support and Prof. A. Böck for providing us with the *E. coli* strain BL21(DE3)cysE51. Discussions with Dr. H.-J. Schirra are gratefully acknowledged. This project was supported by an ETH research grant to R.G.

References

- [1] Holmgren, A. and Björnstedt, B. (1995) *Methods Enzymol.* 252, 199–209.
- [2] Martin, J.L. (1995) *Structure* 3, 245–250.
- [3] Grauschopf, U., Winther, J.R., Korber, P., Zander, T.P., Dallinger, P. and Bardwell, J.C.A. (1995) *Cell* 83, 947–955.
- [4] Huber-Wunderlich, M. and Glockshuber, R. (1998) *Fold. Des.* 3, 161–171.
- [5] Mössner, E., Huber-Wunderlich, M. and Glockshuber, R. (1998) *Protein Sci.* 7, 1233–1244.
- [6] Hol, W.G.J. (1985) *Prog. Biophys. Mol. Biol.* 45, 149–195.
- [7] Jeng, M.F., Holmgren, A. and Dyson, H.J. (1995) *Biochemistry* 34, 10101–10105.
- [8] Gane, P.J., Freedman, R.B. and Warwicker, J. (1995) *J. Mol. Biol.* 249, 376–387.
- [9] Kortemme, T., Darby, N.J. and Creighton, T.E. (1996) *Biochemistry* 35, 14503–14511.
- [10] Nelson, J.W. and Creighton, T.E. (1994) *Biochemistry* 33, 5974–5983.
- [11] Szajewski, R.P. and Whitesides, G.M. (1980) *J. Am. Chem. Soc.* 102, 2011–2026.
- [12] Dyson, H.J., Jeng, M.F., Tennant, L.L., Slaby, I., Lindell, M., Cui, D.S., Kuprin, S. and Holmgren, A. (1997) *Biochemistry* 36, 2622–2636.
- [13] Kallis, G.B. and Holmgren, A. (1980) *J. Biol. Chem.* 255, 10261–10265.
- [14] Li, H., Hanson, C., Fuchs, J.A., Woodward, C. and Thomas, G.J.J. (1993) *Biochemistry* 32, 5800–5808.
- [15] Vohnik, S., Hanson, C., Tuma, R., Fuchs, J.A., Woodward, C. and Thomas Jr., G.J. (1998) *Protein Sci.* 7, 193–200.
- [16] Takahashi, N. and Creighton, T.E. (1996) *Biochemistry* 35, 8342–8353.
- [17] Chivers, P.T., Prehoda, K.E., Volkman, B.F., Kim, B.M., Markley, J.L. and Raines, R.T. (1997) *Biochemistry* 36, 14985–14991.
- [18] Müller, S., Senn, H., Gsell, B., Vetter, W., Baron, C. and Böck, A. (1994) *Biochemistry* 33, 3404–3412.
- [19] Griffey, R.H. and Redfield, A.G. (1985) *Biochemistry* 24, 817–822.
- [20] Riesenberger, D., Menzel, K., Schulz, V., Schumann, K., Veith, G., Zuber, G. and Knorre, W.A. (1990) *Appl. Microbiol. Biotechnol.* 34, 77–82.
- [21] Markley, J.L., Bax, A., Arata, Y., Hilbers, C.W., Kaptein, R., Sykes, B.D., Wright, P.E. and Wüthrich, K. (1998) *Pure Appl. Chem.* 70, 117–142.
- [22] Güntert, P., Dötsch, V., Wider, G. and Wüthrich, K. (1992) *J. Biomol. NMR* 2, 619–629.
- [23] Bartels, C., Xia, T., Billeter, M., Güntert, P. and Wüthrich, K. (1995) *J. Biomol. NMR* 6, 1–10.
- [24] LeMaster, D.M. (1996) *Biochemistry* 35, 14876–14881.
- [25] Dyson, H.J., Gippert, G.P., Case, D.A., Holmgren, A. and Wright, P.E. (1990) *Biochemistry* 29, 4129–4136.
- [26] Jung, G., Breitmeier, E. and Voelter, W. (1972) *Eur. J. Biochem.* 24, 438–445.
- [27] Rost, J. and Rapoport, D. (1964) *Nature* 201, 185.
- [28] Chivers, P.T., Prehoda, K.E. and Raines, R.T. (1997) *Biochemistry* 36, 4061–4066.
- [29] Wunderlich, M., Otto, A., Maskos, K., Mücke, M., Seckler, R. and Glockshuber, R. (1995) *J. Mol. Biol.* 247, 28–33.
- [30] Nordstrand, K., Aslund, F., Meunier, S., Holmgren, A., Otting, G. and Berndt, K.D. (1999) *FEBS Lett.* 449, 196–200.
- [31] Creighton, T.E. (1993) in: *Proteins: Structures and Molecular Properties*, pp. 162–165, Freeman, New York.
- [32] Kirby, A.J. (1980) *Adv. Phys. Org. Chem.* 17, 183–278.